

Vortex rings and vortex ring solitons in shaken Bose-Einstein condensate

V.I. Yukalov¹, A.N. Novikov^{1,2}, E.P. Yukalova³, and V.S. Bagnato²

¹Bogolubov Laboratory of Theoretical Physics, Joint Institute for Nuclear Research, Dubna 141980, Russia

²Instituto de Física de São Carlos, Universidade de São Paulo, CP 369, 13560-970 São Carlos, São Paulo, Brazil

³Laboratory of Informational Technologies, Joint Institute for Nuclear Research, Dubna 141980, Russia

E-mail: yukalov@theor.jinr.ru

Abstract. In a shaken Bose-Einstein condensate, confined in a vibrating trap, there can appear different nonlinear coherent modes. Here we concentrate on two types of such coherent modes, vortex ring solitons and vortex rings. In a cylindrical trap, vortex ring solitons can be characterized as nonlinear Hermite-Laguerre modes, whose description can be done by means of optimized perturbation theory. The energy, required for creating vortex ring solitons, is larger than that needed for forming vortex rings. This is why, at a moderate excitation energy, vortex rings appear before vortex ring solitons. The generation of vortex rings is illustrated by numerical simulations for trapped ⁸⁷Rb atoms.

1. Introduction

Nonlinear Schrödinger (NLS) equation exhibits different kinds of soliton-like solutions. Various solitonic solutions are well known for the NLS equation in nonlinear optics [1, 2] and in Bose-Einstein condensates [3, 4]. The behavior of solitons in both these nonlinear media possesses many common features [5, 6].

Here we concentrate on two types of solutions to the NLS equation, vortex ring solitons and vortex rings. The theoretical study of such solutions is usually based on the assumption of their existence at the initial moment of time, after which one considers their temporal dynamics starting from the given initial condition. In a realistic situation, in order to create a soliton in a Bose-condensed system, it is necessary to apply an external perturbation rendering the condensate strongly nonequilibrium. There are several ways of perturbing the system. Trap rotation or laser rotation inside a trap is known to produce quantum vortices and vortex lattices [7]. To generate a variety of other coherent modes, it has been suggested [8–10] to shake the condensed system, which can be realized either by trap shaking [8–11] or by scattering length modulation [12, 13]. A special variant of a double-loop pattern of laser stirring [14] shows the effect similar to trap shaking.

Ring dark solitons are known in optics [15] and in Bose-Einstein condensate [8–11, 16, 17]. Ring vortex solitons can be stable for weak atomic repulsion, but become unstable for sufficiently strong effective repulsion, such as is typical for trapped atoms. However, their lifetime can be rather long, of order of seconds, which allows one to treat them as metastable objects [18, 19].

Note that bright vortex solitons, existing for attractive atomic interactions, are unstable in three dimensions [20, 21].

In the presence of external perturbations, vortex ring solitons experience snake instability [22] and can split into multiple fragments [19], and finally decay into vortex rings [23, 24]. A reconnection between vortex lines can also lead to the emission of vortex rings [25, 26].

In the present paper, we consider the situation, when Bose-condensed trapped atoms are subject to an external perturbation, which corresponds to trap shaking. The setup is explained in Sec. 2. Such trap shaking can generate different nonlinear coherent modes, including vortices and ring vortex solitons [8–11]. The definition of coherent modes, as stationary solutions to the NLS equation, is given in Sec. 3. When the effective coupling parameter is asymptotically small, it is possible to approximate the solutions to the NLS equation by Gauss-Laguerre modes. We show that, even for arbitrarily strong coupling parameter, nonlinear coherent modes can be well characterized by Hermite-Laguerre modes, provided the description is done by means of optimized perturbation theory [27, 28].

In our previous papers [29–32], we have demonstrated that by shaking a trapped Bose-Einstein condensate, we can generate the following nonequilibrium states: weak nonequilibrium, vortex state, vortex turbulence, grain turbulence, and wave turbulence. Analyzing now in more detail the initial stage of weak nonequilibrium, we numerically simulate the three-dimensional NLS equation and find out that, when no special resonance conditions are involved, in the regime of moderately strong perturbations, vortex rings arise. This happens yet before vortices start appearing in the vortex stage and far before vortex turbulence develops. The results of the numerical simulation, observing vortex rings, are presented in Sec. 4.

To summarize, in the present paper we show the following:

(i) We demonstrate that vortex ring solitons, that are a particular case of nonlinear coherent modes, can be characterized as Hermite-Laguerre modes, provided optimized perturbation theory is used. By vortex ring solitons, we understand circular dark solitons with circulation around the trap axis.

(ii) A vortex ring is defined as a circular line of zero density, with circulation around each of its elements. By numerical simulations, we show that a moderate trap shaking produces vortex rings in a trapped ^{87}Rb .

(iii) We explain why vortex rings arise before vortex ring solitons and even before vortices. This is because the generation of vortex rings requires much less energy than that needed for the creation of other nonlinear coherent modes, including vortices and vortex ring solitons.

2. Shaken trap setup

We consider Bose atoms in a trap described by the harmonic trap potential

$$U(\mathbf{r}) = \frac{m}{2} (\omega_{\perp}^2 r_{\perp}^2 + \omega_z^2 r_z^2) , \quad (1)$$

where $r_{\perp}^2 = r_x^2 + r_y^2$ is the radial spatial variable and r_z is the longitudinal spatial variable. The trap aspect ratio is

$$\alpha \equiv \frac{\omega_z}{\omega_{\perp}} = \left(\frac{l_{\perp}}{l_z} \right)^2 . \quad (2)$$

Atoms interact through the local interaction potential

$$\Phi(\mathbf{r}) = \Phi_0 \delta(\mathbf{r}) , \quad \Phi_0 \equiv 4\pi\hbar^2 \frac{a_s}{m} , \quad (3)$$

where m is atomic mass and a_s , scattering length. The strength of interactions is characterized by the dimensionless coupling parameter

$$g \equiv 4\pi N \frac{a_s}{l_{\perp}} , \quad (4)$$

where N is the number of atoms.

Temperature is assumed to be low, so that almost all atoms are in the Bose condensed state. The shape of the atomic cloud in the trap can be estimated in the Thomas-Fermi approximation [7], which yields the cloud radius

$$R = 1.036 l_{\perp} (\alpha g)^{1/5} \quad (5)$$

and the cloud length

$$L = \frac{2R}{\alpha} = 2.072 \frac{l_{\perp}}{\alpha} (\alpha g)^{1/5} . \quad (6)$$

Hence the cloud volume is

$$V = \pi R^2 L = 6.986 \frac{l_{\perp}^3}{\alpha} (\alpha g)^{3/5} . \quad (7)$$

Trap shaking is accomplished by imposing an additional time-dependent potential, resulting in the total potential

$$U(\mathbf{r}, t) = U(\mathbf{r}) + V(\mathbf{r}, t) \quad (8)$$

consisting of the stationary confining potential $U(\mathbf{r})$ and an alternating potential $V(\mathbf{r}, t)$. The latter is chosen so that to vibrate the trap without rotation. The shaking potential has the form

$$V(\mathbf{r}, t) = \frac{m}{2} \Omega_x^2(t) (x' - x'_0)^2 + \frac{m}{2} \Omega_y^2(t) (y' - y'_0)^2 + \frac{m}{2} \Omega_z^2(t) (z' - z'_0)^2 , \quad (9)$$

with the vibration frequencies

$$\Omega_{\alpha}(t) = A_{\alpha} \omega_{\alpha} [1 - \cos(\omega t)] . \quad (10)$$

The primed variables x' , y' , and z' are shifted and tilted with respect to the original spatial variables x , y , and z , as is explained in Ref. [33].

3. Vortex ring solitons

Vortex ring solitons are a particular case of nonlinear coherent modes that can be introduced as solutions to the NLS equation possessing a circulation around the trap axis, characterized by a nonzero winding number. Coherent modes can be generated by strongly shaking a trap. In a cylindrical trap, coherent modes can be represented as Hermite-Laguerre modes, which can be done not only for weak interactions, but for any strong atomic interactions, provided *Optimized Perturbation Theory* [27, 28] is employed.

Stationary states of Bose-condensed atoms are described by the stationary NLS equation

$$\hat{H}[\eta]\eta(\mathbf{r}) = E\eta(\mathbf{r}) , \quad (11)$$

with the nonlinear Hamiltonian

$$\hat{H}[\eta] = - \frac{\hbar^2 \nabla^2}{2m} + U(\mathbf{r}) + \Phi_0 |\eta(\mathbf{r})|^2 . \quad (12)$$

The normalization condition for the condensate function is

$$\int |\eta(\mathbf{r})|^2 d\mathbf{r} = N . \quad (13)$$

It is convenient to introduce the dimensionless spatial variables

$$r \equiv \frac{r_{\perp}}{l_{\perp}} , \quad z \equiv \frac{r_z}{l_{\perp}} \quad (14)$$

and the dimensionless condensate function

$$\eta(\mathbf{r}) \equiv \sqrt{\frac{N}{l_{\perp}^3}} \psi(r, \varphi, z). \quad (15)$$

Then, with the dimensionless Hamiltonian

$$\hat{H}[\psi] \equiv \frac{\hat{H}[\eta]}{\hbar\omega_{\perp}}, \quad (16)$$

the eigenvalue problem (11) reads as

$$\hat{H}[\psi_{nmj}] \psi_{nmj}(r, \varphi, z) = E_{nmj} \psi_{nmj}(r, \varphi, z). \quad (17)$$

Here

$$\hat{H}[\psi] \equiv -\frac{1}{2} \nabla^2 + \frac{1}{2} (r^2 + \alpha^2 z^2) + g |\psi|^2, \quad (18)$$

with

$$\nabla^2 = \frac{\partial^2}{\partial r^2} + \frac{1}{r} \frac{\partial}{\partial r} + \frac{1}{r^2} \frac{\partial^2}{\partial \varphi^2} + \frac{\partial^2}{\partial z^2}.$$

The normalization condition (13) becomes

$$\int_0^{\infty} r dr \int_0^{2\pi} d\varphi \int_{-\infty}^{\infty} |\psi_{nmj}(r, \varphi, z)|^2 dz = 1. \quad (19)$$

In optimized perturbation theory [27, 28], we start with a trial Hamiltonian

$$\hat{H}_0 = -\frac{1}{2} \nabla^2 + \frac{1}{2} (u^2 r^2 + v^2 z^2) \quad (20)$$

including control functions u and v to be defined from an optimization condition. The trial wave function, corresponding to Hamiltonian (20), is given by the expression

$$\begin{aligned} \psi_{nmj}(r, \varphi, z) &= \left[\frac{2n! u^{|m|+1}}{(n+|m|)!} \right]^{1/2} r^{|m|} \exp\left(-\frac{u}{2} r^2\right) L_n^{|m|}(ur^2) \frac{e^{im\varphi}}{\sqrt{2\pi}} \times \\ &\times \left(\frac{v}{\pi}\right)^{1/4} \frac{1}{\sqrt{2^j j!}} \exp\left(-\frac{v}{2} z^2\right) H_j(\sqrt{v} z), \end{aligned} \quad (21)$$

where L_n^m is a generalized Laguerre polynomial and H_j is a Hermite polynomial. Here $n = 0, 1, 2, \dots$ is a radial quantum number, $m = 0, \pm 1, \pm 2, \dots$ is an azimuthal quantum number or the winding number of circulation, and $j = 0, 1, 2, \dots$ is an axial quantum number.

The optimization condition, defining the control functions, can be chosen in several forms, the simplest of which is

$$\left(\delta u \frac{\partial}{\partial u} + \delta v \frac{\partial}{\partial v} \right) \left(\psi_{nmj}, \hat{H}[\psi_{nmj}] \psi_{nmj} \right) = \left(\delta u \frac{\partial}{\partial u} + \delta v \frac{\partial}{\partial v} \right) E_{nmj} = 0. \quad (22)$$

The spectrum of coherent modes is

$$E_{nmj} = \frac{p}{2} \left(u + \frac{1}{u} \right) + \frac{q}{4} \left(v + \frac{\alpha^2}{v} \right) + \frac{u\sqrt{v}}{(2\pi)^{3/2}} J_{nmj} g, \quad (23)$$

in which

$$p \equiv p_{nm} = 2n + |m| + 1, \quad q \equiv q_j = 2j + 1 \quad (24)$$

and

$$J_{nmj} \equiv \frac{(2\pi)^{3/2}}{u\sqrt{v}} \int |\psi_{nmj}(r, \varphi, z)|^4 r dr d\varphi dz. \quad (25)$$

The optimization condition (22) gives the equations for the control-functions:

$$p \left(1 - \frac{1}{u^2}\right) + \frac{G}{\alpha p} \sqrt{\frac{v}{q}} = 0, \quad q \left(1 - \frac{\alpha^2}{v^2}\right) + \frac{uG}{\alpha p \sqrt{vq}} = 0, \quad (26)$$

where we define the effective coupling parameter

$$G \equiv G_{nmj} = \frac{2p\sqrt{q}}{(2\pi)^{3/2}} J_{nmj} \alpha g. \quad (27)$$

In a typical situation with trapped atoms, the effective coupling is strong, such that

$$g \gg 1, \quad G \gg 1. \quad (28)$$

Then the control functions are

$$u \simeq \frac{p}{G^{2/5}}, \quad v \simeq \frac{\alpha^2 q}{G^{2/5}}. \quad (29)$$

We are interested in the radial shape of the condensate density. To this end, we set $j = 0$ and define the radial density

$$\rho_{nm}(r) \equiv \int |\psi_{nm0}(r, \varphi, z)|^2 d\varphi dz,$$

for which we obtain

$$\rho_{nm}(r) = \frac{2n! u^{m+1}}{(n+m)!} r^{2m} \exp(-ur^2) [L_n^m(ur^2)]^2, \quad (30)$$

where $m \geq 0$.

The effective coupling parameter is

$$G = \frac{2p}{(2\pi)^{3/2}} J_{nm} \alpha g \quad (q = 1),$$

with

$$J_{nm} \equiv \frac{1}{u} \int_0^\infty \rho_{nm}^2(r) r dr.$$

In particular,

$$\begin{aligned} J_{00} &= 1, & J_{01} &= \frac{1}{2}, & J_{02} &= \frac{3}{8}, \\ J_{10} &= \frac{1}{2}, & J_{11} &= \frac{5}{16}, & J_{12} &= \frac{1}{4}, \\ J_{20} &= \frac{11}{32}, & J_{21} &= \frac{15}{64}, & J_{22} &= \frac{199}{1024}. \end{aligned}$$

In Figs. 1, 2, and 3, we present the radial density of coherent modes for different quantum numbers. The radial number n defines the number of nodes, while the winding number m characterizes circulation. For numerical calculations, we accept the parameters as in our previous experiments with ^{87}Rb , described in Refs. [29–33], where

$$\alpha = 0.11, \quad g = 1.96 \times 10^4, \quad \alpha g = 2.156 \times 10^3.$$

For comparison, we present vortex solutions, with nonzero m , and non-circulating solutions, with $m = 0$.

4. Generation of vortex rings

The typical radii of rings appearing in a trap are much larger than the coherence length l_c and, clearly, smaller than the trap radius R ,

$$r_R \gg l_c, \quad r_R < R. \quad (31)$$

The coherence length

$$l_c \equiv \frac{\hbar}{mc} = \frac{1}{\sqrt{4\pi\rho a_s}} \quad \left(c = \frac{\hbar}{m} \sqrt{4\pi\rho a_s} \right) \quad (32)$$

defines the vortex ring core.

Ring characteristics can be estimated resorting to the Thomas-Fermi approximation [7]. Normalizing the Thomas-Fermi condensate function yields the condensate energy

$$E_{TF} = \frac{1}{2} \left(\frac{15}{4\pi} \alpha g \right)^{2/5} = 0.5367(\alpha g)^{2/5}$$

expressed in units of $\hbar\omega_\perp$. The condensate density at the trap center reads as

$$\rho(0) = 0.537 \frac{\alpha N}{l_\perp^3 (\alpha g)^{3/5}}.$$

Taking the latter for estimating the coherence length gives

$$l_c = R \sqrt{\frac{4\pi L}{15gl_\perp}} = 1.365 \frac{l_\perp}{(\alpha g)^{1/5}}. \quad (33)$$

The vortex ring characteristics have been considered by Iordanskii [34], Amit and Gross [35], Roberts and Grant [36], and Jones and Roberts [37]. Following Refs. [35, 36], for the energy of a vortex ring, in units of $\hbar\omega_\perp$, we have

$$E_R = 2\pi^2 \rho r_R l_\perp^2 \ln \left(2.25 \frac{r_R}{l_c} \right), \quad (34)$$

where the density ρ is to be taken at the location of the ring.

Since the density is smaller close the boundary of a trapped atomic cloud, we expect that it is easier to create rings close to the boundary, since this requires smaller energy. The following numerical simulations confirm this.

Generally, a vortex ring moves with velocity that, far from the cloud edges, can be estimated as

$$v_R = \frac{\hbar}{2mr_R} \ln \left(6.12 \frac{r_R}{l_c} \right), \quad (35)$$

the velocity being directed perpendicular to the ring plane. The ring possesses a stationary position (although nonequilibrium) when its radius is $r_R \sim 0.6 R$. But in the standard situation the ring has an inherent tendency to propagate along the z axis. In a trap, the ring oscillates [38, 39]. Estimating the period of the ring oscillation [40] one has

$$T_R \sim \frac{4\pi R/l_c}{\omega_z \sqrt{\ln(R/l_c)}}. \quad (36)$$

Substituting here the expressions for R and l_c , we find

$$T_R \sim \frac{4\pi(\alpha g)^{2/5}}{\omega_z \sqrt{\ln(0.5\alpha g)}}. \quad (37)$$

For the accepted setup, where $\omega_z = 2\pi \times 23$ Hz, we get $T_R \sim 0.7$ s.

We accomplish numerical solution of the NLS equation, with the shaking potential (9), using the method of Ref. [41]. It turns out that the first nonequilibrium stage of perturbation, classified in Refs. [30–32] as the regime of weak nonequilibrium, is not as dull. At this stage, there are yet no vortices. However, there appear vortex rings. A vortex ring is defined as a circular line of zero density, with a winding number ± 1 around each of the line elements. Numerically, zero density implies $10^{-8}\rho(0)$. Some typical vortex rings are shown in Fig. 4. Rings usually appear in pairs, so that their total number is even.

In order to understand why vortex rings appear before vortices, we need to compare their energies. The energy of a vortex of length L can be written [7, 31, 32] as

$$E_L = \frac{2\pi}{3} \rho(0) l_\perp^2 L \ln \left(0.949 \frac{R}{l_c} \right), \quad (38)$$

where $\rho(0)$ is the density at the trap center. Since the total number of atoms, in the Thomas-Fermi approximation, is

$$N \equiv \int \rho(\mathbf{r}) d\mathbf{r} = \frac{4\pi}{15} \rho(0) R^2 L, \quad (39)$$

it is also possible to write

$$E_L = \frac{5l_\perp^2}{2R^2} N \ln \left(0.949 \frac{R}{l_c} \right).$$

Comparing the vortex energy (38) with the ring energy (34), we take $r_R \sim 0.6R$, which gives the relation $\rho(r_R) \sim 0.7\rho(0)$ between the atomic density close to the ring location and the density at the center. Then we obtain

$$\frac{E_R}{E_L} \sim \alpha. \quad (40)$$

In the considered setup, $\alpha \sim 0.1$. Hence the ring energy is an order smaller than the vortex energy. Therefore it is much easier to generate vortex rings, requiring to pump into the system much less energy than that needed for producing vortices. It is possible to expect that up to around ten vortex rings could be generated before vortices will start arising. The energy of other coherent modes, including vortex ring solitons is larger than that of basis vortices with the winding number ± 1 . Hence their appearance is even less probable than that of the simple vortices, unless special resonant conditions are imposed.

5. Conclusion

We have analyzed the possibility of creating vortex ring solitons and vortex rings in a shaken Bose-Einstein condensate of trapped atoms. The consideration is based on the NLS equation, assuming that practically all atoms are condensed. Vortex ring solitons are dark solitonic solutions, with circulation around the symmetry axis of the trap. Vortex rings are circular vortices with circulation around each of their elements. Vortex ring solitons can be described analytically by solving the NLS equation using optimized perturbation theory. This solution is valid for an arbitrary strength of atomic interactions, contrary to the simple perturbation theory admissible for only very weak interactions.

Numerical simulation of the three-dimensional NLS equation demonstrates the appearance of vortex rings. This happens in the regime of a rather moderate perturbation, yet before

vortices could arise. That regime corresponds to the weak nonequilibrium stage, according to the classification of Refs. [30–32].

The energy of a vortex ring is essentially smaller than that of a basic vortex with circulation ± 1 . In turn, the energy of a simple vortex is smaller than that of other coherent modes, including vortex ring solitons [42,43]. This explains why, under moderate trap shaking, vortex rings appear long before vortices, since their generation requires much less energy to be injected into the trap. Even if higher-energy coherent modes would be produced at the initial moment of time, they would disintegrate into the lower-energy modes, such as vortices and vortex rings. Vortex rings can also occur in the stage of vortex turbulence [44,45]. However, to reach this regime requires much stronger trap shaking. The investigation of the possible vortex-ring creation under vortex turbulence, realized by trap shaking, is in the progress.

Acknowledgement

Financial support from the Russian Foundation for Basic Research (grant # 14-02-00723) and from the University of São Paulo NAP Program is appreciated.

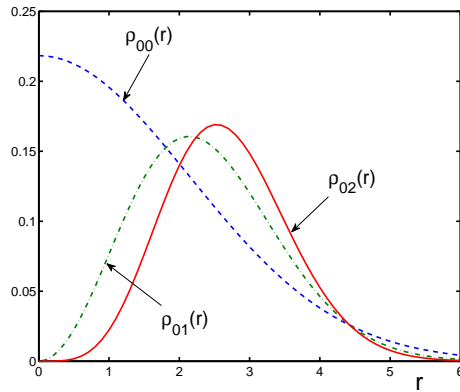


Figure 1. Radial density $\rho_{0m}(r)$ as a function of the dimensionless radius (in units of the transverse oscillator length l_{\perp}). The density of the ground state $\rho_{00}(r)$ (dashed line) is compared with the densities of the vortex states with the winding number $m = 1$ (dashed-dotted line) and $m = 2$ (solid line).

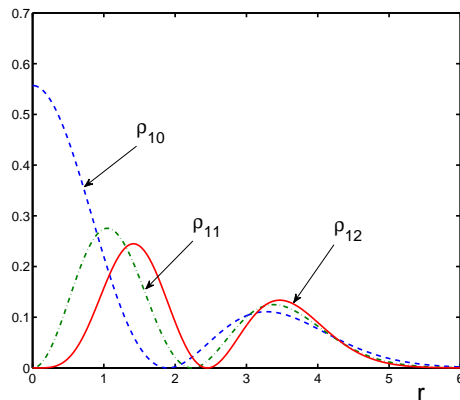


Figure 2. Radial density $\rho_{1m}(r)$ of the ring state $\rho_{10}(r)$ (dashed line), composite vortex + ring states $\rho_{11}(r)$ (dashed-dotted line) and $\rho_{12}(r)$ (solid line).

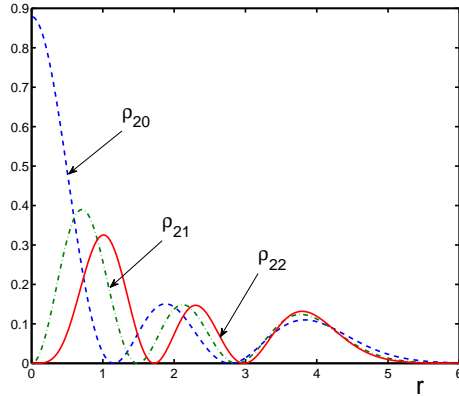


Figure 3. Radial density $\rho_{2m}(r)$ of the double ring state $\rho_{20}(r)$ (dashed line), composite vortex + double-ring states $\rho_{21}(r)$ (dashed-dotted line) and $\rho_{22}(r)$ (solid line).

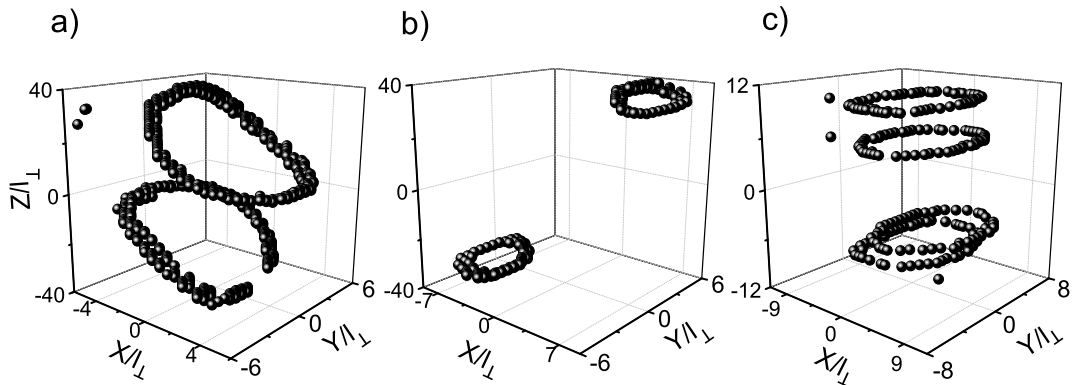


Figure 4. Spatial location of vortex rings after different shaking time: (a) $t = 10.5$ ms; (b) $t = 11$ ms; (c) $t = 14.4$ ms.

- [1] Kivshar Y S and Luther-Davis B 1998 *Phys. Rep.* **298** 81
- [2] Briedis D, Petersen D E, Edmundson D, Krolikowski W, and Bang O 2005 *Opt. Express* **13** 435
- [3] Komineas S 2007 *Eur. Phys. J. Spec. Top.* **147** 133
- [4] Frantzeskakis D J 2010 *J. Phys. A* **43** 213001
- [5] Malomed B A 2006 *Soliton Management in Periodic Systems* (New York: Springer)
- [6] Kartashov Y V, Malomed B A, and Torner L 2011 *Rev. Mod. Phys.* **83** 247
- [7] Pethick C J and Smith H 2008 *Bose-Einstein Condensation in Dilute Gases* (Cambridge: Cambridge University)
- [8] Yukalov V I, Yukalova E P, and Bagnato V S 1997 *Phys. Rev. A* **56** 4845
- [9] Yukalov V I, Yukalova E P, and Bagnato V S 2000 *Laser Phys.* **10** 26
- [10] Yukalov V I, Yukalova E P, and Bagnato V S 2001 *Laser Phys.* **11** 455
- [11] Yukalov V I, Yukalova E P, and Bagnato V S 2002 *Laser Phys.* **12** 231
- [12] Yukalov V I and Bagnato V S 2009 *Laser Phys. Lett.* **6** 399
- [13] Yukalov V I 2011 *Phys. Part. Nucl.* **42** 460
- [14] Allen A J, Parker N G, Proukakis N P, and Barenghi C F 2014 *Phys. Rev. A* **89** 025602
- [15] Kivshar Y S and Yang X 1994 *Phys. Rev. E* **50** 40
- [16] Brand J and Reinhardt W P 2001 *J. Phys. B* **34** L113
- [17] Theocharis G, Frantzeskakis D J, Kevrekidis P G, Malomed B A, and Kivshar Y S 2003 *Phys. Rev. Lett.* **2003** 120403
- [18] Car L D and Clark C W 2006 *Phys. Rev. A* **74** 043613
- [19] Li J, Wang D S, Wu Z Y, Yu Y M, and Liu W M 2012 *Phys. Rev. A* **86** 023628

- [20] Adhikari S K 2003 *New J. Phys.* **5** 137
- [21] Adhikari S K 2004 *Phys. Rev. A* **69** 063613
- [22] Kadomtsev B B and Petviashvily V I 1970 *Phys. Dokl.* **15** 539
- [23] Anderson B P, Haljan P C, Regal C A, Feder D L, Collins L A, Clark C W, and Cornell E A 2001 *Phys. Rev. Lett.* **86** 2926
- [24] Ginsberg N S, Brand J, and Hau L V 2005 *Phys. Rev. Lett.* **94** 040403
- [25] Svistunov B V 1995 *Phys. Rev. B* **52** 3647
- [26] Laurie J and Baggaley A W 2015 *J. Low Temp. Phys.* **180** 95
- [27] Yukalov V I 1976 *Moscow Univ. Phys. Bull.* **31** 10
- [28] Yukalov V I 1976 *Theor. Math. Phys.* **28** 652
- [29] Shiozaki R F, Telles G D, Yukalov V I, and Bagnato V S 2011 *Laser Phys. Lett.* **8** 393
- [30] Yukalov V I, Novikov A N, and Bagnato V S 2014 *Laser Phys. Lett.* **11** 095501
- [31] Yukalov V I, Novikov A N, and Bagnato V S 2015 *J. Low Temp. Phys.* **180** 53
- [32] Yukalov V I, Novikov A N, and Bagnato V S 2015 *Phys. Lett. A* **379** 1366
- [33] Seman J A, Henn E A, Shiozaki R F, Roati G, Poveda-Cuevas F J, Magalhães K M F, Yukalov V I, Tsubota M, Kobayashi M, Kasamatsu K, and Bagnato V S 2011 *Laser Phys. Lett.* **8** 691
- [34] Iordanskii S V 1965 *J. Exp. Theor. Phys.* **21** 467
- [35] Amit D and Gross E P 1966 *Phys. Rev.* **145** 130
- [36] Roberts P H and Grant J 1971 *J. Phys. A* **4** 55
- [37] Jones C A and Roberts P H 1982 *J. Phys. A* **15** 2599
- [38] Jackson B, McCann J F, and Adams C S 1999 *Phys. Rev. A* **61** 013604
- [39] Reichl M D and Mueller E J 2013 *Phys. Rev. A* **88** 053626
- [40] Bulgac A, Forbes M M, Kelley M M, Roche K J, and Wlazlowski G 2014 *Phys. Rev. Lett.* **112** 025301
- [41] Novikov A N, Yukalov V I, and Bagnato V S 2015 *J. Phys. Conf. Ser.* **594** 012040
- [42] Courteille P W, Bagnato V S, and Yukalov V I 2001 *Laser Phys.* **11** 659
- [43] Bagnato V S and Yukalov V I 2013 *Prog. Opt. Sci. Photon.* **1** 377
- [44] Tsubota M, Kobayashi M, and Takeushi H 2013 *Phys. Rep.* **522** 191
- [45] Nemirovskii S R 2013 *Phys. Rep.* **524** 85